

Leaky_relu activation function, CSP1_X, CSP2_X and SPP.

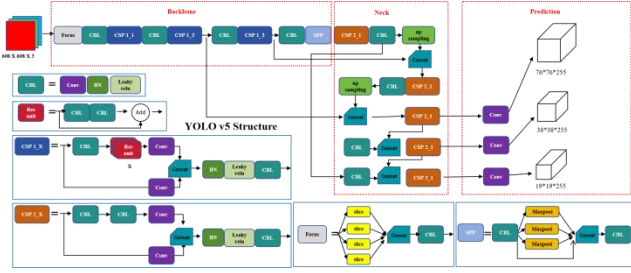


Figure 2. The structure of the YOLOv5 model

Anchor Boxes (Anchor Boxes) are used in YOLOv5 to predict the location and size of objects. The model automatically adjusts the size of the anchor box according to the distribution of the dataset during the training process to improve the detection accuracy. The loss function of the model, Equation (3), consists of Equation (1) localization loss (CIoU), confidence loss, and Equation (2) classification loss.

$$CIoU = 1 - IoU + \frac{\rho^2(b, b_{gt})}{c^2} + \alpha v \quad (1)$$

where IoU is the intersection ratio between the predicted and real frames, $\rho^2(b, b_{gt})$ is the distance between the centroids, c is the size of the enclosing frame, v is the difference in aspect ratios, and α is used to balance the various losses.

$$FL(p_i) = -\alpha_i(1 - p_i)^\gamma \log(p_i) \quad (2)$$

where p_i is the class probability predicted by the model, α_i is used to control the focus on difficult-to-categorize samples, and γ is a penalty factor, usually set to 2.

$$\text{Total Loss} = \lambda_{box} \cdot CIoU + \lambda_{cls} \cdot FL_{cls} + \lambda_{obj} \cdot FL_{obj} \quad (3)$$

where λ_{box} , λ_{cls} , and λ_{obj} are hyperparameters that regulate the contribution of different losses to the total losses

Contrastive Loss: Contrastive Loss is a loss function for metric learning that aims to train a model so that pairs of similar samples are brought as close as possible in the feature space and pairs of dissimilar samples are moved as far away as possible. The core goal is to learn the similarity and dissimilarity between samples in such a way that similar pairs of samples are mapped to regions close together and dissimilar pairs are mapped to regions far away in the embedding space (typically the feature space of a deep neural network). The contrast loss function improves the feature representation, and by optimizing the contrast loss, the model learns to distinguish more between different classes of features, the mathematical formulation of which is shown in Equation 4.

$$L_{contrastive} = \frac{1}{2N} \sum_{i=1}^N [y_i \cdot \max(0, m - d(x_i, x_j))^2 + (1 - y_i) \cdot d(x_i, x_j)^2] \quad (4)$$

where $d(x_i, x_j)$ is the distance between samples x_i and x_j , usually using the Euclidean distance: $d = \|x_i - x_j\|^2$, m denotes the minimum distance that needs to be maintained between samples of different categories, y_i is the label, $y_i=1$ means that the two samples are similar, $y_i=0$ means that the two samples are not

similar, and N is the total number of sample pairs.

3. FBSSDA Attention

FBSSDA (Foreground-Background Same-Scale Difference Attention) attention is a technique inspired by the distinction between foreground and background features in image processing tasks. In order to distinguish between foreground and background features of an image and to obtain features containing significant differences between them, a new FBSSDA attention for extracting the differences between foreground and background features at the same scale of an image is proposed. FBSSDA attention is obtained by letting the weight of the relative values of the background features and the features of the candidate region be added to the object attention score, and then extracting the feature vectors of the foreground and the background regions separately and solving the difference, and obtaining the feature vectors containing significant differences between the two. a feature that contains the significance difference between the two. Such features contain some of the feature space information of the background and affect the subsequent calculation of the object attention score value for that region.

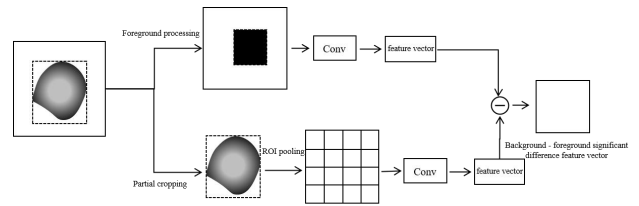


Figure 3. FBSSDA Attention Diagram

The FBDF attention is shown in Figure 3, and its main processing flow is as follows: (i)input the image into the feature extraction network to get the compressed feature map F ; (ii)multiply the fixed mask M with the feature map F to get the background feature map $F_b=M \times F$ containing only the features of the non-candidate regions; (iii)perform the convolution operation on the background feature map to get the compressed background feature vector $\alpha=f(F_b)$; (iv)crop the candidate region locally from the feature map F and use the region of interest pooling to obtain the local feature map F_f ; (v)perform the convolution operation on the local feature map to obtain the compressed local feature vector $\beta=f(F_f)$; (vi)calculate the significant difference value on the feature vectors obtained from the third and the fifth steps to obtain the feature vector $\Theta=|\alpha-\beta|$ that contains the background-foreground disparity features.

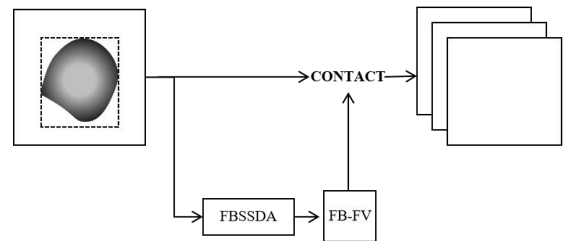


Figure 4. FBSSDA Feature Fusion Module

4. YOLOv5 model based on FBSSDA attention

In order to solve the problem of unknown defects in the production process of industrial panels, we proposed a new attention FBSSDA method and constructed a feature fusion module consisting of FBSSDA attention as shown in Figure 4,

and added this module into the YOLOv5 model to construct an improved YOLOv5 model called FBSSDA-YOLOv5 model. In Figure 4, the FBSSDA attention module outputs feature vectors(FB-FV) of background-foreground disparity features to be fused with the original image to enhance foreground features.

The structure of the FBSSDA-YOLOV5 model is shown in Fig. 5, where the FBSSDA feature fusion module is used to perform feature fusion on the outputs of the Neck layer of the YOLOv5 model for subsequent predictive classification. In order to better learn the differences between similar samples, the contrast loss function is introduced, which makes the object features of the same category more similar and the object features of different categories more different, which can make the unknown defects easier to be detected and defined. After introducing the contrast loss function, the loss function of the FBSSDA-YOLOV5 model is shown in Equation 5.

$$\text{Total Loss} = \lambda_{\text{box}} \cdot \text{CIoU} + \lambda_{\text{cls}} \cdot \text{L}_{\text{cls}} + \lambda_{\text{obj}} \cdot \text{L}_{\text{obj}} + \lambda_{\text{contrastive}} \cdot \text{L}_{\text{contrastive}} \quad (5)$$

In display panel defect detection scenarios, there is a common problem of an unbalanced number of categories, which can lead to worse fitting of the already difficult-to-balance multiclassification model. Based on the One-vs-ALL strategy, converting the multicategorization problem into multiple binary classification problems reduces the difficulty of model fitting and allows the model to better distinguish different categories in the feature space, although it brings overhead in computation and storage costs.

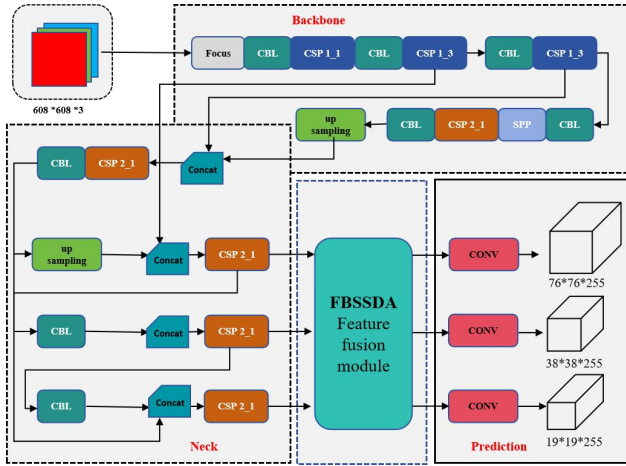


Figure 5. FBSSDA-YOLOv5 model structure diagram

The operation logic of multiclassification to biclassification is shown in Figure 6, and the steps are as follows: (i)input the picture into the network model to get the original output, and the third dimension of the output consists of 4 (box predicted value), 1 (obj predicted value) and N (category predicted value), in which W_i stands for the predicted value of the i th category (non-probability);(ii)calculate the probability of the i th category by taking the maximal value of the other categories as the noni predicted value, denoted as $W_j = \max(W_p)$, where $p \neq i$; (iii)use the sigmoid function to convert W_i and W_j into P_i (the probability of category i), where $P_i \in (0,1)$; (iv)repeat steps 2 and 3 to calculate the probability of the other categories and the probability of non-that category; (v)take the probability of the maximum value of all the categories, P_{\max} , and the probability of the maximum value of the non-that category, Q_{\max} . If

$P_{\max} > Q_{\max}$, the output P_{\max} is the final output class confidence. If $P_{\max} \leq Q_{\max}$, the output $1-Q_{\max}$ is the final output class confidence.

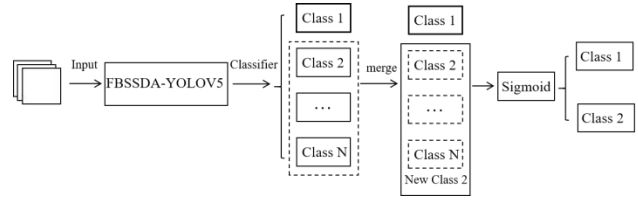


Figure 6. Schematic diagram of the steps for converting a multiclassification to a dichotomous classification

In model forward propagation, since the non-maximal suppression (NMS) algorithm usually relies on a fixed threshold (e.g., IoU threshold) to determine whether to remove redundant frames or not, there exists a significant drawback: it is unable to deal with the unknown defects efficiently, and the detection algorithms are not capable of detecting the features or morphology of defects that have not been learned in the real industrial production. Therefore, the U-NMS algorithm is proposed in the post-processing stage of the algorithm, which improves the NMS algorithm by introducing an uncertainty measure. The steps of the algorithm are (i) to sort all candidate frames based on their confidence scores; (ii) to select the frame B_{\max} with the highest confidence score as the current frame; (iii) to compute the IoU and uncertainty attenuation between frames, and for each candidate frame B_j overlapping with B_{\max} , to decide whether to suppress the frame or not based on its IoU and uncertainty metrics; and (iv) to dynamically through the uncertainty to adjust the IoU threshold; (v) repeat steps (ii) to (iv) until all candidate boxes are processed. In step (ii), IoU attenuation is to calculate the IoU values of the current frame and other candidate frames, and if $\text{IoU}(B_{\max}, B_j)$ is greater than a certain threshold (which can be dynamically adjusted by uncertainty), the attenuation process continues. Uncertainty decay is for each candidate box B_j , calculate its uncertainty difference with the current box B_{\max} as shown in Equation 6:

$$\text{uncertainty}(B_{\max}, B_j) = \sigma_j - \sigma_{\max} \quad (6)$$

where σ_{\max} is the uncertainty measure of the current frame B_{\max} . If the $\text{uncertainty}(B_{\max}, B_j)$ of a candidate frame is small, it means that the frame has a high similarity with the current frame, and its confidence can be further adjusted by uncertainty attenuation:

$$\text{score}_j = \text{score}_j \cdot \exp\left(-\frac{\text{IoU}(B_{\max}, B_j)^2}{\alpha + \sigma_j^2}\right) \quad (7)$$

where α is a hyperparameter that controls the degree of combination of IoU and uncertainty decay.

In addition, the predictive logic of the model is also modified and its operational logic is shown in Figure 7 with the steps:(i)input the image, and get the original output after the calculation of the model; (ii)calculate the obj confidence of the current candidate region and the class confidence of each known category, respectively; (iii)judge whether the obj confidence satisfies the threshold condition, and if it does not satisfied, judge that the candidate region is background, if so, go to the next step; (iv)judge whether ClassConfidence satisfies the

threshold condition, if so, judge that the candidate region is a known category defect, if not, go to the next step; (v)extract the probability of not being of that category (background) in step (iv) of the Improvement Point II, calculate the mean squared deviation of the probability values of class confidence and each not being of that category, and calculate the mean squared deviation of the probability values of class confidence and each not being of that category. Class confidence and the maximum of the mean square difference value of each non-that class probability value is the background feature distance; (vi)judge whether the distance obtained in the previous step satisfies the condition, if it does, determine the region as a suspected unknown class defect region and output the prediction result, if it does not satisfy the condition, determine it as a background region.

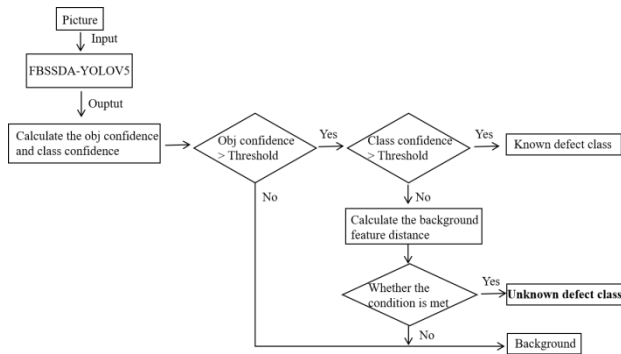


Figure 7. Improving YOLOv5 Network Feature Space and Detection Logic

5. Display panel unknown defect detection and analysis examples

Display panel unknown defect detection process: Unknown defect detection in pictures of display panels, the design of the unknown defect interception algorithm flowchart shown in Figure 8, first from the object detection algorithm to determine a certain class of pictures, to find defective pictures, and the over-detection rate needs to be controlled in a certain range; taking into account the ease of maintenance of the algorithm in the later stages, the algorithm needs to try to cover all the products of all the sites, i.e., a set of parameter adaptation of all the detection; the algorithm needs to be The algorithm needs to re-determine the results of this category of pictures, which accounts for a high percentage, so the reasoning time can not be too long, so as not to affect the operational efficiency.

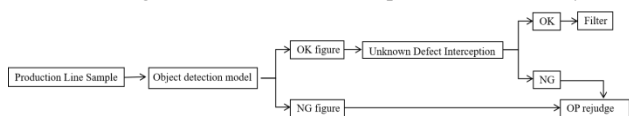


Figure 8. Flowchart of Unknown Defect Interception

Display panel unknown defect detection: In order to validate the accuracy and effectiveness of the algorithm, this paper uses 26309 Mura images provided by the actual production department of the production line for training and testing. The batch of images contains 10 categories of known defects. During the validation process, the batch of images is divided into two parts, 6906 and 19403. To further validate the algorithm's effectiveness in actual production, 42,131 Mura images are specifically collected for inference.

The results detected by the FBSSDA-YOLOv5 model, which

introduces the unknown defect interception algorithm in the first part of the pictures, are compared with the original algorithm YOLOv5, and a comparison of the results is shown in Table 1. Among them, 28 pictures were judged as OK by the object detection algorithm, but were detected as NG in the interception algorithm, and the ADC algorithm over-detection was increased from 559 to 1386, an increase of 827 (not confirmed whether it is a personnel omission), indicating that the interception algorithm can effectively reduce the omission, but the over-detection is increased by a larger amount.

Table 1. FBSSDA-YOLOv5 and YOLOv5 detection results

Mura(6906)	FBSSDA-YOLOv5		YOLOv5	
	OK	NG	OK	NG
True-OK	4563	1386	5390	559
True-NG	14	943	42	943

Table 2. Improved FBSSDA-YOLOv5 detection results

Mura(19403)	FBSSDA-YOLOv5		
	OK	NG	UNKNOWN
True-OK	13133	2886	1094
True-NG	10	1846	434

The FBSSDA-YOLOv5 model was further improved by extracting defects with high object scores but low classification scores as unknown defects from the model and verified in the second part of the images, the results of which are shown in Table 2. A total of 10 images were judged as OK by the algorithm, but were manually detected as NG in the second part. The interception algorithm detected 434 defects and over-detected 1,094 (not confirmed in the second part), with an overall manual substitution rate of 67.74% and a missed detection rate of 0.539%.



Figure 9. FBSSDA-YOLOv5 modeling of poor interception effect diagrams.

The interception effect of the improved FBSSDA-YOLOv5 model on the provided Mura images is shown in Figure 9. At the same time, the model is also deployed to the production line for defect detection for three consecutive days, and its accuracy is 93.48%, 90%, and 98.51%, respectively, corresponding to the number of detected and real defects of 46/43, 30/27, 67/66, and the effect of interception of some unknown defects is shown in Figure 10.

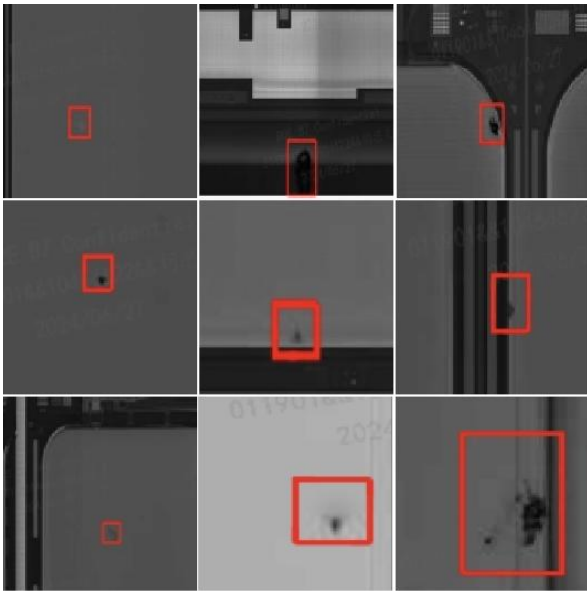


Figure 10. Interception effect of unknown defects on line for FBSSDA-YOLOv5 model.

Finally, the YOLOv5 model was also compared with the FBSSDA-YOLOv5 model 42131 Mura images for practical reasoning, and the comparison of the reasoning results for the OTHER category defects is shown in Table 3. The FBSSDA-YOLOv5 model shows an improvement in the detection of the OTHER category defects in the metrics of mAP-50, which suggests that the model can significantly increase the number of unknown defect identification and improve the confidence level of defects, and the proposed model has a very obvious improvement in the accuracy and recall of OTHER category defects.

Table 3. Results of mAP comparison between YOLOv5 and FBSSDA-YOLOv5 model for OTHER category defects

	Presion	Recall	mAP-50	mAP-95
YOLOv5	0.906	0.829	0.896	0.775
FBSSDA-YOLOv5	0.922	0.843	0.905	0.777

6. Conclusion

Aiming at the problem that the YOLO-based model algorithm cannot effectively recognize the unknown defects leading to missed detection in the actual defect detection scenarios of display panels, a defect detection method based on the improved

YOLOv5 model with FBSSDA attention fusion is proposed to solve the problem of unknown category defect detection in panels. The method has the following characteristics:

1. FBSSDA attention is proposed to increase the weight of background-foreground differences. This method can enhance the extraction ability of the foreground-background difference features, which makes the feature display of defects more obvious.
2. The FBSSDA-YOLOv5 model is proposed, where foreground and background difference features are extracted by FBSSDA attention, and a contrast loss function is added to expand the differences between different defect categories during training. Then for category discrimination, the multicategorization is converted to dichotomous classification, i.e., known defects and unknown defects, based on the One-vs-ALL strategy. In the post-processing session, U-NMS is used to compensate for the disadvantage that NMS cannot detect unknown defects, and the prediction logic is updated. This method is more capable of detecting unknown defects than the original YOLOv5 model, and is now used in the production of display panel processes.

The improved YOLOv5 method based on FBSSDA attentional fusion used in the defect detection process can also be widely applied to the process production of other display panels and also to other industrial.

7. References

1. He, F., Tan, J., Wang, W., Liu, S., Zhu, Y., & Liu, Z. (2023). EFFNet: Element-wise feature fusion network for defect detection of display panels. *Signal Processing: Image Communication*, 119, 117043.
2. Redmon, J. (2016). You only look once: Unified, real-time object detection. In *Proceedings of the IEEE conference on computer vision and pattern recognition*.
3. Almufareh, M. F., Imran, M., Khan, A., Humayun, M., & Asim, M. (2024). Automated brain tumor segmentation and classification in MRI using YOLO-based Deep Learning. *IEEE Access*.
4. Benjumea, A., Teeti, I., Cuzzolin, F., & Bradley, A. (2021). YOLO-Z: Improving small object detection in YOLOv5 for autonomous vehicles. *arXiv preprint arXiv:2112.11798*.
5. Pham, D. L., & Chang, T. W. (2023). A YOLO-based real-time packaging defect detection system. *Procedia Computer Science*, 217, 886-894.